Freezing effects of oil-in-water emulsions studied by sum-frequency scattering spectroscopy

W. J. Smit,[1, a)] N. Smolentsev,[2] J. Versluis,[1] S. Roke,[2] and H. J. Bakker[1]

[1)]*FOM Institute AMOLF, Science Park 104, 1098 XG Amsterdam, The Netherlands*

[2)]*Laboratory for Fundamental Biophotonics (LBP), Institute of Bioengineering (IBI),*
School of Engineering (STI), École Polytechnique Fédérale de Lausanne (EPFL), 1015 Lausanne,
Switzerland.

(Dated: 18 July 2016)

Temperature-dependent sum-frequency scattering spectroscopy is used to study the properties of hexadecane and dodecane oil droplets in water. The sum-frequency scattering spectra contain vibrational bands that correspond to the symmetric and antisymmetric CH stretching vibrations of the methylene (CH_2) and methyl (CH_3) groups of the alkane molecules. The relative amplitudes of the vibrational bands provide information on the surface structure and the shape of the oil droplets. We study the sum-frequency scattering spectra over a temperature range of -48 to $24\,°C$, including the freezing transitions of the water matrix and the oil droplets. Hexadecane oil droplets freeze at a higher temperature than the surrounding water, whereas dodecane oil droplets freeze at a lower temperature than the surrounding water. This allows us to independently study the freezing effect of oil and water on the surface structure of the oil droplets. In both cases, freezing leads to a change in the polarization dependencies that are valid in the case of the spherical-symmetric shapes that the oil droplets assume when both water and oil are liquid. We find that the freezing of water leads to a strong distortion of the liquid dodecane surface but has little effect on the surface of already solidified hexadecane. For completely frozen emulsions a further decrease in temperature is observed to lead to a further distortion of the surface of the solid oil particles, which might be caused by increasing hardness of the ice matrix encapsulating the particles.

I. INTRODUCTION

Oil-in-water emulsions are omnipresent in oil-based products, including foods, cosmetics, paints, crop protectors, and pharmaceuticals.[1–3] The emulsion properties are determined by the molecular-scale structure of the adjacent oil and water layers, as this structure determines the free energy of the oil–water interface. The freezing of oil-in-water emulsions affects many functional properties like their stability[4], which is relevant in many applications, for instance in the chilled storage of frozen ready meals. Previously the liquid–solid phase transitions of emulsified oils have extensively been studied with differential scanning calorimetry[4–9] and ultrasonics[10–13]. The bulk properties of frozen emulsified oils have been investigated with X-ray scattering experiments[14–16] and electron microscopy[17]. However, until now no direct study on the molecular structure of the oil droplet surface upon freezing has been performed. To this purpose, temperature-dependent sum-frequency scattering is a powerful technique.

Recently, sum-frequency scattering made it possible to obtain information about the molecular structure of the oil droplet–water interface.[18,19] Sum-frequency scattering is an interface specific technique in which a broadband infrared (IR) laser pulse is overlapped with a narrow visible (VIS) beam in a solution with dispersed particles. When the centrosymmetry is broken (for instances at interfaces) a second-order polarization can be created that oscillates at the sum-frequency of the incoming beams: $\omega_{SF} = \omega_{VIS} + \omega_{IR}$. The sum-frequency (SF) signal is only generated at the droplet interfaces for liquid oil droplets in liquid water. The efficiency of the SF generation is strongly enhanced when the IR frequency ω_{IR} coincides with a vibrational resonance. Hence, the spectral shape and strength of the SF scattering signal provide unique information about the surface structure.[20,21,22] Until now, no temperature-dependent SF scattering study has been reported.

In this study, we develop temperature-dependent SF scattering and use this technique to monitor the effects of phase changes on the interface of oil-in-water emulsions. We investigate two oil-in-water emulsions: a hexadecane-in-water emulsion with the oil freezing temperature above the freezing point of water, and a dodecane-in-water emulsion with the oil freezing temperature below the freezing point of water.[4] We present and discuss SF scattering spectra at room temperature and at different temperatures during cooling down to $-48\,°C$.

II. EXPERIMENT

The SF scattering experiments are performed using a commercial Ti:sapphire laser system (Coherent Evolution) that delivers 3.2 mJ pulses at a wavelength of 800 nm (FWHM 70 nm) and at a repetition rate of 1 kHz. The VIS pulse is made by spectrally narrowing 20 % of the laser output to a FWHM of 0.6 nm (10 cm^{-1}) by a pulse shaper[23]. The IR pulse is generated using a home-

built Optical Parametric Amplifier (OPA), pumped by the other 80 % of the laser output. This process yields 20 μJ pulses at 3.4 μm (2900 cm^{-1}) with a FWHM bandwidth of 280 nm (240 cm^{-1}). The polarizations of the VIS and IR light are independently adjusted by a combination of a $\lambda/2$-plate and a polarizer.

A schematic of the experimental geometry is shown in Fig. 1. The IR and VIS light are focused by the same 90° off-axis parabolic gold mirror with an effective focal length of 10 cm to a spot size of about 150 μm and are incident under a relative angle of 6° (as measured in air). To match the focused spot sizes of the IR and VIS beams[24], the VIS beam size is reduced by a telescope before the parabolic mirror.

The SF scattering signal is collected by a collimating lens with a focal distance of 4 cm under an angle of 45° and an effective diameter of 23 mm, corresponding to an acceptance angle of 21–41° of the SF signal of a water sample. A shortpass filter (Semrock FF01-775/SP-25) and bandpass filter (Semrock FF02-650/100-25) are used to suppress background scattering of the VIS beam and light generated at other frequencies by higher order processes. A final polarizer cube is used to select the polarization of the SF light. The SF light is detected by a Princeton Instruments spectrometer system consisting of a Pixis 100 CCD camera in conjunction with an Acton SP 2356 monochromator. We use an integration time of 300 s per spectrum.

The sample is cooled in two stages. A processor cooler (LD PC-V2) with a cooling power of 300 W at −30 °C
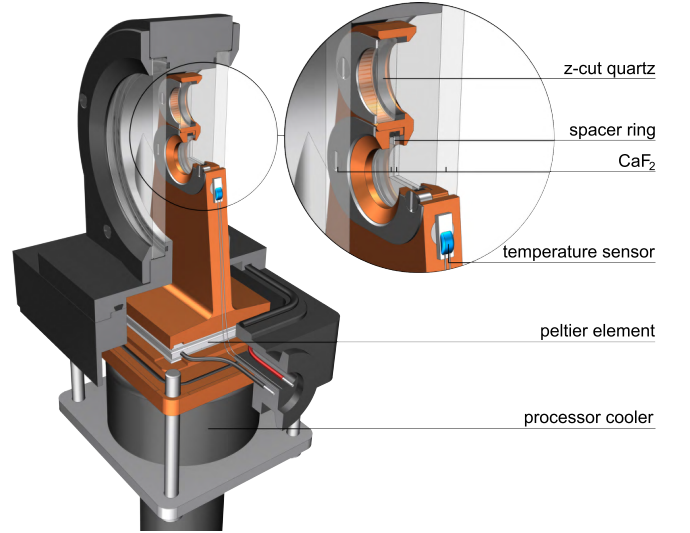

FIG. 2. Schematic drawing of the sample cell holder.

cools a copper board on which a 40 W double stage Peltier element is mounted. On top of the Peltier element a movable copper holder is placed, which can hold an emulsion between two Raman grade CaF$_2$ windows (Crystran) with a 100 μm spacer and a z-cut quartz crystal (see Fig. 2). The copper holder is held in place by a flexible spring steel plate which acts as a pressure release. By adjusting the current through the Peltier element, temperatures down to −60 °C can be achieved. During the experiments, we used a cooling rate of maximally 2 °C/min. In order to prevent condensation on the windows of the sample cell holder, the last part of the setup is enclosed and continuously purged with dry nitrogen.

Recorded SF spectra are shown as a function of IR frequency in units of wavenumber (cm^{-1}). The spectra are baseline subtracted and corrected for the air–CaF$_2$ reflection losses in s-polarization. The polarization combinations are given in order of decreasing frequency of the interacting light fields, i.e. ssp stands for s-polarized SF, s-polarized VIS, and p-polarized IR light. For spherical liquid droplets the non-zero polarization configurations are ppp, ssp, sps, and pss, and the latter two have nearly identical spectral shapes.[25] All spectra are normalized to a SF spectrum of z-cut quartz measured in reflection geometry in the ssp-polarization combination in order to divide out the spectral shape of the IR beam[26]. We switched between measuring emulsions in the scattering geometry and quartz reference spectra by shifting the height of our sample cell holder (see Fig. 2).

The emulsions are prepared by adding 1 vol% dodecane or 2 vol% hexadecane to a solution of 10 mM deuterated sodium dodecyl sulfate (SDS) in D$_2$O. Hexadecane and dodecane are from Sigma–Aldrich and have analytical purity ($\geq$ 99.8 %). Deuterated SDS (98 % D) is obtained from Cambridge Isotopes and D$_2$O (99.8 % D) from Armar Chemicals. The emulsions are ultrasonicated
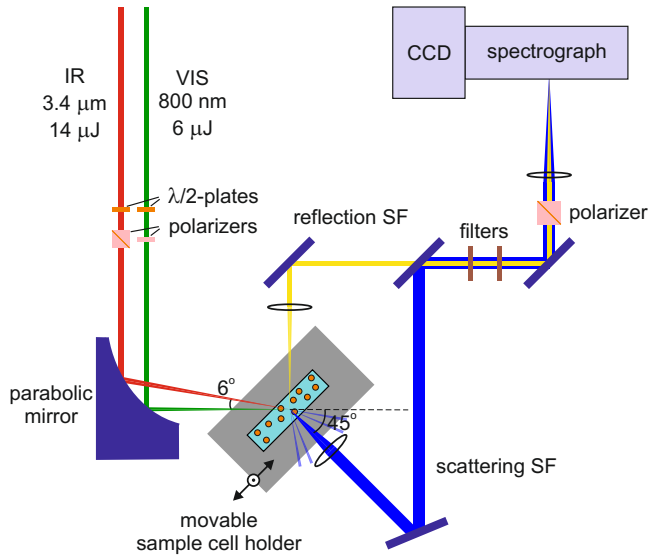

FIG. 1. Schematic of the experimental setup. An IR beam (red) and a VIS beam (green) are collimated by the same parabolic mirror and overlapped in the sample cell containing an emulsion. SF scattered light (blue) is generated in a wide angular range. A collimating lens selects an angular range which is conducted into the spectrograph. The reflection detection scheme, which is used for referencing of the IR spectrum, is indicated in yellow.
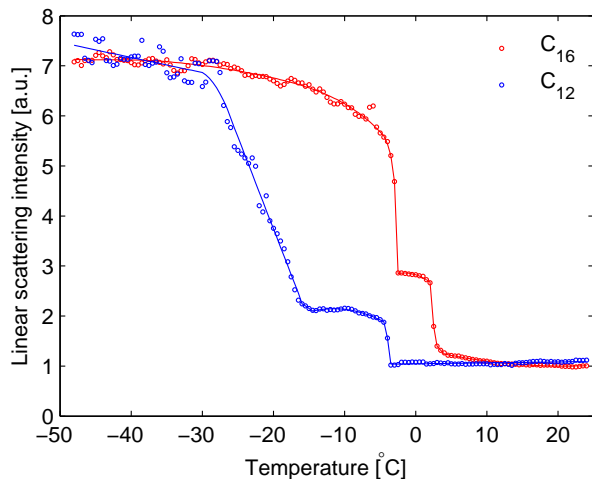
FIG. 3. Temperature dependence of the linear scattering intensity of a diode laser for the C_{16} and C_{12} emulsions by cooling from 24 to $-48\,^{\circ}C$. Intensity changes are an indicator of phase transitions.

to decrease the average droplet radii, which is characterized by dynamic light scattering (using a Malvern Zetasizer Nano ZS) to be 116 ± 21 nm for the hexadecane emulsion and 59 ± 14 nm for the dodecane emulsion. Both emulsions have a surface to volume ratio of about 5×10^5 m^{-1} in the hard sphere approximation. The addition of SDS makes the emulsions stable, even over years[27]. With the droplet concentrations used the scattering is in the linear regime[19], multiple scattering will thus be negligible. Hereafter, we will denote the hexadecane-in-D_2O emulsion as the C_{16} emulsion and the dodecane-in-D_2O emulsion as the C_{12} emulsion after the number of carbon atoms in the alkane.

Due to supercooling, the freezing temperatures in emulsions are lower than in bulk, which are reported to be $3.8\,^{\circ}C$ for D_2O, $18.1\,^{\circ}C$ for hexadecane, and $-9.6\,^{\circ}C$ for dodecane.[28] We measure the freezing transition temperatures of the C_{16} and C_{12} emulsions by linear light scattering,[29,30] shown in Fig. 3. During the linear light scattering experiment the water phase crystallizes rapidly in the whole sample at -3 and $-4\,^{\circ}C$ for the C_{16} and C_{12} emulsion, respectively. However, given that the water solvent can nucleate from a single nucleation core, the water crystallization temperature can vary by a couple of degrees, even for samples of the same composition.[6,31] The oil droplet solidification takes place over a broad range due to the polydispersity in droplet size[5,9,10]. This finding agrees with differential scanning calorimetry experiments.[4] The oil solidification takes place in the C_{16} emulsion from 2.5 to $1\,^{\circ}C$ and in the C_{12} emulsion over a broader temperature range from -15 to $-27\,^{\circ}C$.[32]
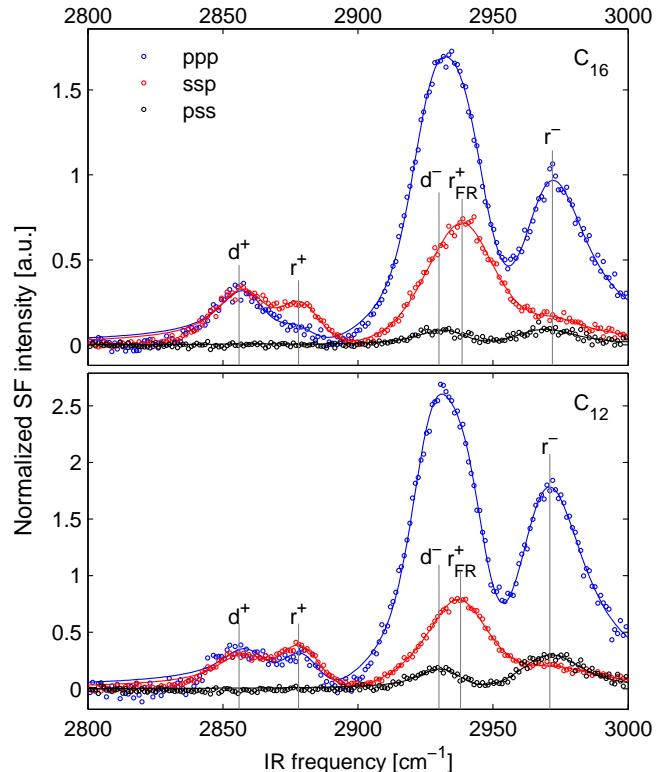
III. RESULTS AND DISCUSSION

A. Room temperature

FIG. 4. SF scattering spectra of the liquid–liquid interface of the C_{16} emulsion (top) and the C_{12} emulsion (bottom) at $24\,^{\circ}C$. Circles represent experimental data points and solid lines are fitted curves to the experimental data (see text). The different CH_2 and CH_3 modes are indicated by their abbreviations.

Figure 4 shows SF scattering spectra of the two alkane-in-water emulsions taken at room temperature. The different polarization combinations allows to assign the resonances. Similar to reflective SF[33], one can formulate rules of thumb for the dependence of the scattering SF signals on the polarization configuration. For our experimental configuration, the following dependencies on the polarization configurations are expected:[20,34]

(a) Symmetric CH_2 and CH_3 vibrations are stronger in the *ssp*- than in the *ppp*-polarization combination and negligible in the *pss*-polarization combination.

(b) Antisymmetric CH_2 and CH_3 vibrations are strongest in the *ppp*-, intermediate in the *pss*-, and weakest in the *ssp*-polarization combination.

Therefore, we can assign the symmetric CH_2 stretch mode (d^+, at ~ 2857 cm^{-1}), the symmetric CH_3 stretch mode (r^+, at ~ 2878 cm^{-1}), and the nearly degenerate antisymmetric CH_3 stretch mode (r^-, at ~ 2970 cm^{-1}). The

antisymmetric CH_2 stretch mode (d^-, at ~ 2928 cm^{-1}) overlaps with a Fermi Resonance of the r^+ with the overtone of the antisymmetric bending vibration (r^+_{FR}, at ~ 2940 cm^{-1}).[35,36] In the *pss*-polarization combination the d^- dominates and in the *ssp*-combination the r^+_{FR} dominates. In the *ppp*-polarization combination both the d^- and the r^+_{FR} are strong and they are observed as a single broad band. The deviation of a few wavenumbers with other literature values[18,34,36–38] falls within the uncertainty in the calibration of the spectrometer.

The solid lines in Fig. 4 are fits with five Lorentzian-shaped resonances and a spectral width of 10 cm^{-1} for the visible beam. The explicit formula is given in Eq. (S6) of the Supplemental Material.[22] To decrease the covariant noise in the fitting procedure, we assumed the resonance widths of the CH_2 and CH_3 symmetric stretch vibrations to be equal.

An alkane molecule with an even number of carbon atoms in an all-*trans* configuration has local inversion symmetry at the centre of each C–C bond. Therefore, symmetry considerations impose that no SF photons can be emitted from the symmetric CH_2 stretch (d^+) vibration of an alkane in all-*trans* conformation.[39] Therefore, the amplitude ratio of the d^+ and the r^+ vibrations is a measure of the deviation from an all-*trans* conformation of the alkyl chains.[18,38–43] In the *ssp*-polarization combination we find a d^+/r^+ ratio of 0.49 ± 0.14 for the C_{12} emulsion and a d^+/r^+ ratio of 0.89 ± 0.13 for the C_{16} emulsion. The latter is in agreement with the value of 0.88 ± 0.42 found by de Aguiar et al.[18] It follows that the d^+/r^+ ratio is 1.8 ± 0.6 times larger for hexadecane than for dodecane. Thus, hexadecane molecules have more gauche defects than dodecane molecules, which agrees with their difference in alkyl chain length. This ratio is in reasonable agreement with reflective SF studies on the liquid alkane–air interface by Esenturk et al.[43] where the d^+/r^+ amplitude ratio (as determined from the intensity ratio) was found to be 1.12 ± 0.07 for dodecane and 1.8 ± 0.3 for hexadecane.

The d^+/r^+ ratio depends on the polarization combination. In the *ppp*-polarization combination we find a d^+/r^+ ratio of 1.6 ± 0.4 for the C_{16} emulsion and 0.76 ± 0.13 for the C_{12} emulsion. The d^+/r^+ ratios in the *ppp*-polarization combination are thus 1.8 ± 0.4 (hexadecane) and 1.6 ± 0.2 (dodecane) times higher than in the *ssp*-polarization combination. This result agrees with calculations using the theoretical framework provided by de Beer and Roke[20], predicting the d^+/r^+ ratio to be 1.5 times larger in the *ppp*- than in *ssp*-polarization combination.

The antisymmetric CH_3 stretch (r^-) and symmetric CH_3 stretch (r^+) vibrations both originate from the same part of the alkane molecule and the r^-/r^+ amplitude ratio gives information about the average molecular tilt of the end group.[34] In the *ssp*-polarization combination we find a r^-/r^+ ratio of 0.38 ± 0.15 for the C_{16} emulsion and 0.26 ± 0.07 for the C_{12} emulsion. Calculations by Chen et al.[34] show that these ratios correspond to average tilt an-

gles of the CH_3 group with respect to the droplet surface normal of $30 \pm 30°$ for the C_{16} emulsion and $55 \pm 15°$ for the C_{12} emulsion[34]. The r^-/r^+ ratio strongly depends on the polarization combination.
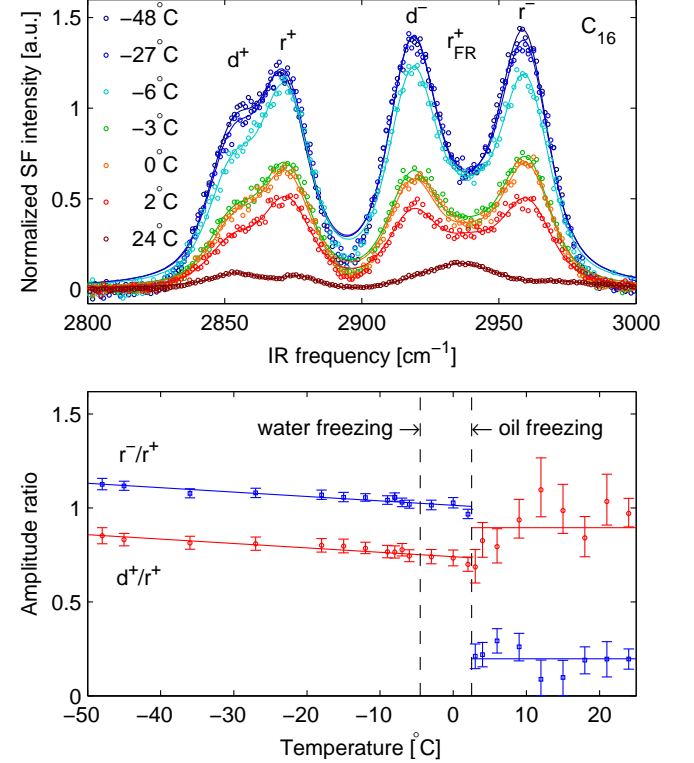
B. C_{16} emulsion freezing

FIG. 5. Top: SF scattering spectra in the *ssp*-polarization combination of the C_{16} emulsion at a selection of temperatures by cooling from 24 to $-48\,°C$. Circles represent experimental data points and solid lines are fits based on five resonances (see text). Bottom: The d^+/r^+ (red) and r^-/r^+ (blue) amplitude ratios of the C_{16} emulsion as determined by the fitting procedure. The dashed lines are the freezing points of the water and the oil. Error bars represent 95 % confidence intervals of the spectral fitting procedure and the solid lines are trends.

In the top panel of Fig. 5 we present SF scattering spectra in the *ssp*-polarization configuration at a selection of temperatures. For the liquid emulsion, we do not observe any significant changes in the amplitude and shape of the SF scattering spectra when we vary the temperature. The spectrum at $24\,°C$ represents an average of several SFS spectra measured in the liquid phase. This spectrum is fitted using Eq. (S6).[22]

When we cool the C_{16} emulsion down to $-48\,°C$, we observe discontinuous intensity increments in the SF scattering signal at temperatures that correspond with the phase transition temperatures (Fig. 3). The oil solidification, visible from $2\,°C$, induces both spectral changes
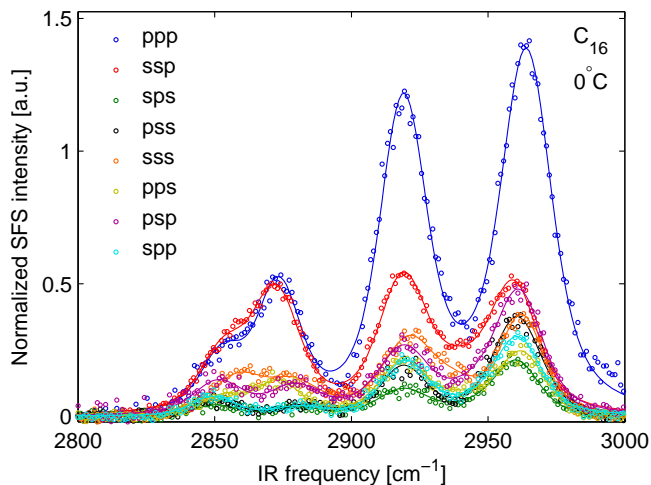
FIG. 6. SF scattering spectra for all eight possible polarization combinations of the C_{16} emulsion at $0\,^\circ$C with frozen oil droplets and liquid water. SF scattering signal is observed for all eight polarization combinations, indicating less strict polarization selection rules than for the spherical symmetric droplets in the liquid emulsion (see text).

as well as an overall increase in SF intensity. Note that the bulk crystal structure of frozen hexadecane is triclinic pinacoid[6,44] which is centrosymmetric and thus SF forbidden. Hence, the changes in SF spectrum are manifestations of the interfacial changes.

The formation of crystallites leads to an increase in the SF intensity as a result of (a combination of) the following three effects:

1. Ordering of the alkyl chains at the interface.[45]

2. Deviations from the spherical shape of liquid oil droplets leading to a larger interfacial area.[25,46]

3. The formation of multiple crystalline domains per frozen oil droplet. At the interfaces of the crystalline domains the symmetry is broken and additional SF light can be generated.[47]

Effects 2 and 3 additionally lead to an increase in the SF signal due to a relaxation of the polarization selection rules[25,47], i.e. more second-order susceptibility elements are non-zero than for spherical symmetric droplets. The random crystal orientation of the frozen oil droplets also contributes to the relaxation of the polarization selection rules.[47] The relaxation of the polarization selection rules is confirmed by the fact that oil freezing results in the observation of SF signal for all eight polarization configurations (Fig. 6). Combined molecular dynamics and quantum-chemical calculations would be required to determine the relative importance of these effects.

As oil freezing can result in a large variety of particles with different shapes, crystal orientations, and crystalline domains, the effective surface second-order susceptibility that determines the SF response of a particle can be different for each particle. To obtain structural informa-

tion, we fit the intensity spectra with an incoherent sum of Lorentzians, representing the d^+, r^+, d^-, r^+_{FR} and r^- bands. More details on the fitting and the d^+, r^+, and r^- amplitudes are given in the Supplemental Material.[22] The d^+/r^+ and r^-/r^+ amplitude ratios are shown in the bottom panel of Fig. 5.

The crystallization of the hexadecane oil droplets leads to an increase of the r^-/r^+ ratio from 0.38 ± 0.15 to 0.96 ± 0.03 at $2\,^\circ$C. The value of 0.38 is observed for the all-liquid phase for which there is no polarization mixing. This r^-/r^+ ratio corresponds to an average tilt angle of the terminal CH_3 group of $30\,^\circ$C.[34] The r^-/r^+ ratio of 0.96 observed at $2\,^\circ$C cannot be related to a tilt angle as there is strong polarization mixing (Fig. 6), leading to a significant *ppp*-type signal for an *ssp*-polarization combination configuration. The d^+/r^+ ratio is observed to decrease from 0.89 ± 0.13 to 0.70 ± 0.04 at $2\,^\circ$C, which tentatively indicates an enhanced ordering and a decrease of the number of gauche defects of the hexadecane molecules at the interface. A decrease of the d^+/r^+ ratio has also been found in the case of hexadecane freezing at a hexadecane–sapphire interface.[48] However, as freezing also leads to a change of the polarization selection rules, it is not possible to draw unambiguous structural conclusions from the change in d^+/r^+ ratio.

The freezing of the water matrix at $-4\,^\circ$C does not lead to an abrupt change in the shape of the SF spectrum: neither the d^+/r^+ nor the r^-/r^+ ratio changes. This observation implies that water freezing has no effect on the shape and surface structure of already solid oil particles. This can be explained from the fact that the ice matrix is not very solid just below the freezing point: apparently the amorphous liquid-like layers of water molecules at the ice-oil interface fully accommodate the shape of the frozen oil droplets. This scenario is illustrated in the top panel of Fig. 9. The freezing of the water matrix does lead to an increase in the intensity of the SF signal. This is likely an effect of the clustering of the oil particles induced by the water freezing[1,4,49] because clustered oil particles scatter SF light at much higher intensities than isolated particles[46,50].

When the temperature is further decreased, the d^+/r^+ and r^-/r^+ ratios both gradually increase. The d^+/r^+ ratio increases from 0.74 ± 0.03 at $-6\,^\circ$C to 0.85 ± 0.04 at $-48\,^\circ$C. The r^-/r^+ ratio increases from 1.02 ± 0.02 at $-6\,^\circ$C to 1.13 ± 0.03 at $-48\,^\circ$C. The increase of these ratios indicates that the oil particles become more distorted with decreasing temperature. This can be explained by a hardening of the liquid-like water layer on the ice surface with decreasing temperature.[51]

C. C_{12} emulsion freezing

We also cool the C_{12} emulsion down to $-48\,^\circ$C. The SF scattering spectra at a selection of temperatures during the cooling process are shown in the top panel of Fig. 7. The spectra for the liquid emulsion do not show
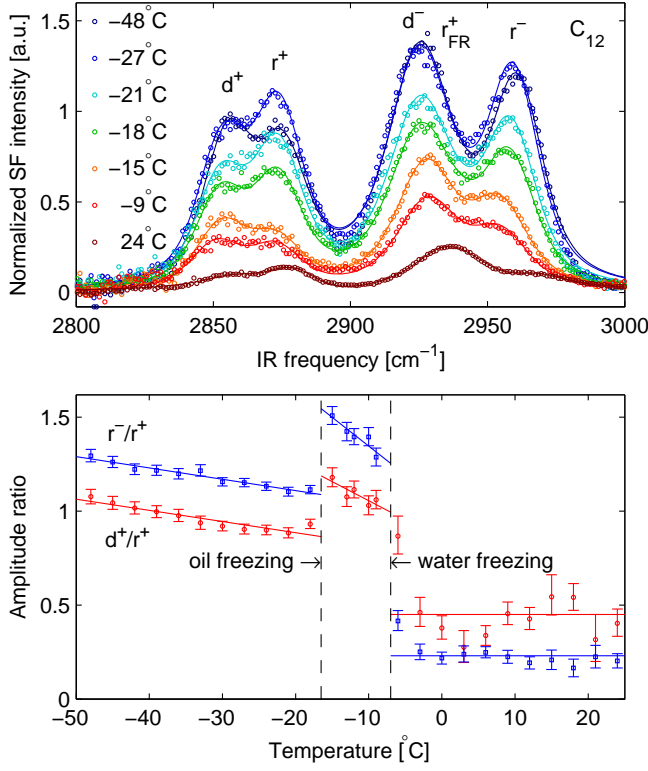
FIG. 7. Top: SF scattering spectra in the *ssp*-polarization combination of the C_{12} emulsion at a selection of temperatures by cooling from 24 to $-48\,^{\circ}$C. Circles represent experimental data points and solid lines are fits based on five resonances (see text). Bottom: The d^+/r^+ (red) and r^-/r^+ (blue) amplitude ratios of the C_{12} emulsion as determined by the fitting procedure. The dashed lines are the freezing points of the oil and the water. Error bars represent 95 % confidence intervals of the spectral fitting procedure and the solid lines are trends.

any significant changes as a function of temperature. The spectrum at 24 $^{\circ}$C represents an average of the several SF scattering spectra measured in the liquid phase, which is fitted using Eq. (S6).[22]

For the C_{12} emulsion the water phase freezing occurs at $-7\,^{\circ}$C with the oil still being liquid. This causes an increases in SF intensity, which is likely a result of the clustering of the oil droplets.[1,4,49] Since we observe scattered SF photons for all eight polarization combinations (Fig. 8) which is not allowed for spherical droplets, we conclude that the water freezing induces a strong deformation of the liquid oil droplets[25], probably as a result of the water expansion upon freezing. The water freezing likely leads to a large variety of droplet shapes, each with their own effective second-order susceptibility. We fit the intensity spectra with an incoherent sum of five Lorentzians as we did for the C_{16} emulsion with frozen oil droplets. The resulting amplitudes of the d^+, r^+, and r^- resonances are shown in Fig. S1.[22] The d^+/r^+ and r^-/r^+ amplitude ratios are shown in the bottom panel of Fig. 5. Both the d^+/r^+ and r^-/r^+ ratios increase upon
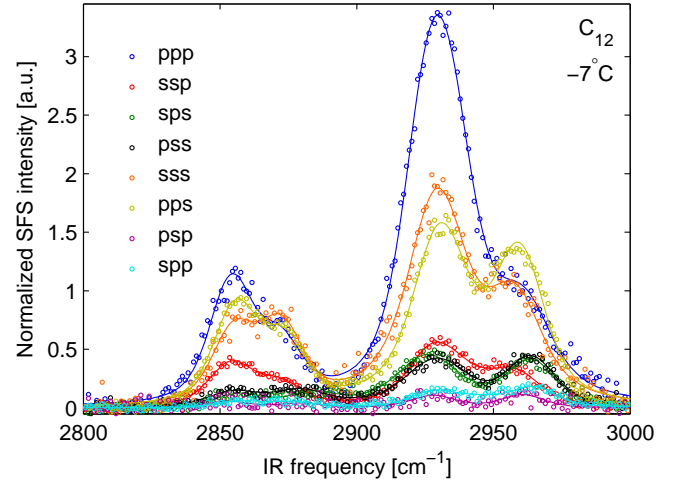

FIG. 8. SF scattering spectra for all eight possible polarization combinations of the C_{12} emulsion at $-7\,^{\circ}$C with a frozen water phase and liquid oil droplets. SF signal is observed for all eight polarization combinations, indicating non-spherical droplet shapes.

freezing. At $-9\,^{\circ}$C the r^-/r^+ ratio is 1.29 ± 0.04. The increase of the r^-/r^+ ratio follows from the deformation of the oil droplets induced by the frozen water matrix. Freezing of the water matrix also leads to an increase of the d^+/r^+ ratio from 0.49 ± 0.14 to 1.06 ± 0.05 at $-9\,^{\circ}$C. This change is likely due to an increase in the number of gauche defects of the dodecane molecules at the droplet interface. However, it may in part also result from the modification of the polarization dependencies due to the fact that the droplets become non-spherical. A strong increase of the d^+/r^+ and the r^-/r^+ ratios is observed in the temperature range from -9 down to $-15\,^{\circ}$C, which can be explained from a hardening of the ice matrix, leading to a stronger deformation of the liquid oil droplets.

The dodecane oil droplets freeze at temperatures below $-17\,^{\circ}$C. The solidification of the oil droplets leads to larger SF signals and the crystallization causes a modification in the polarization dependencies, like we observed for the C_{16} emulsion. The oil solidification is accompanied by a decrease in oil volume[52,53] and is observed to lead to a decrease of the r^-/r^+ ratio from 1.51 ± 0.05 at $-15\,^{\circ}$C to 1.11 ± 0.02 at $-18\,^{\circ}$C, which indicates that the surface deformation that was induced by the freezing of the water matrix gets somewhat reduced when the oil freezes. The bottom illustration of Fig. 9 illustrates this scenario. The d^+/r^+ ratio decreases from 1.18 ± 0.05 at $-15\,^{\circ}$C to 0.93 ± 0.03 at $-18\,^{\circ}$C. This observation tentatively shows that the freezing of the oil leads to an increased ordering of the dodecane alkyl chains thereby decreasing the number of gauche defects and thus the d^+/r^+ ratio. A further decrease of the temperature again increases both the d^+/r^+ ratio and the r^-/r^+ ratio. This observation indicates that the surface of the oil particle becomes more distorted at lower temperatures. As in the case of the C_{16} emulsion, this effect is probably caused

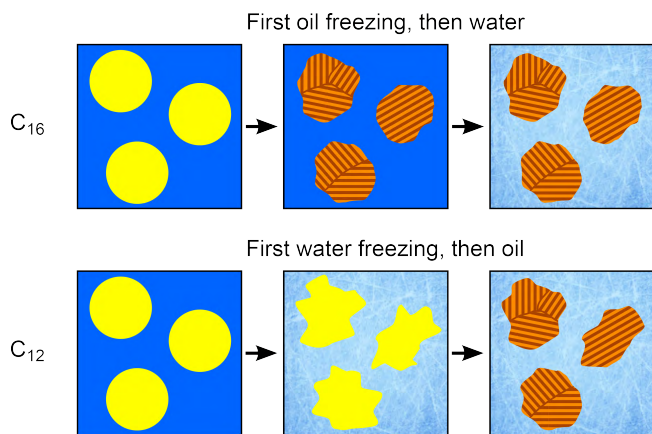by the hardening of the ice matrix with decreasing temperature.

First oil freezing, then water

First water freezing, then oil

FIG. 9. Illustration of the effect of a decrease in temperature on the oil droplets for the C_{16} emulsion (top) and the C_{12} emulsion (bottom). The liquid–solid transitions are indicated by the black arrows. Freezing of the water matrix has very little effect when the oil is solid (C_{16} emulsion) and a large influence on the oil droplet surface when the oil is liquid (C_{12} emulsion). Freezing of the oil droplets in liquid water leads to a distortion of the spherical droplet surface (C_{16} emulsion), whereas freezing of dodecane oil droplets in ice reduces the distortion that resulted from the freezing of the water matrix (C_{12} emulsion).

In the temperature range where the oil droplets are frozen, the r^-/r^+ ratio is larger for the C_{12} emulsion than for the C_{16} emulsion. This finding indicates that the frozen dodecane droplets are stronger deformed than the frozen hexadecane particles.

IV. CONCLUSIONS

We studied the molecular interfacial properties of hexadecane and dodecane oil droplets in aqueous emulsions with sum-frequency scattering spectroscopy in the temperature range from 24 to $-48\,°C$ temperatures including the water–ice and liquid–solid oil transitions. The SF scattering spectra show vibrational bands corresponding to the symmetric CH_2 vibration (d^+), the antisymmetric CH_2 vibration (d^-), the symmetric CH_3 vibration (r^+) and its Fermi resonance (r^+_{FR}), and the antisymmetric CH_3 vibration (r^-). The d^+/r^+ and the r^-/r^+ amplitude ratios provide information on the conformation of the alkane molecules and the shape of the oil droplets. Both oil and water freezing lead to a distortion of the spherical-symmetry of the droplets and a modification of the polarization dependencies, which in turn affects the d^+/r^+ and r^-/r^+ ratios. Whereas the freezing of hexadecane oil droplets in liquid water leads to changes in the oil surface, the subsequent freezing of the water phase has little effect on the oil surface, probably because the amorphous liquid-like ice layer at the ice–oil interface is soft in

comparison to the surface of already frozen oil droplets. Freezing of the water matrix is observed to lead to a strong distortion of the surface of the oil droplets in case the oil is liquid (dodecane). Freezing of liquid dodecane oil droplets within an ice matrix reduces the distortion that resulted from freezing of the water matrix. Further decreasing the temperature for solid oil particles embedded in ice leads to a further distortion of the oil surface, probably because the ice matrix hardens at lower temperatures, thereby imposing a stronger deformation of the solid oil particle.

[1] B. M. Degner, C. Chung, V. Schlegel, R. Hutkins, and D. J. McClements, Compr. Rev. Food Sci. F. **13**, 98 (2014).
[2] S. Arima, S. Ueno, A. Ogawa, and K. Sato, Langmuir **25**, 9777 (2009).
[3] D. J. McClements, Adv. Colloid Interface Sci. **174**, 1 (2012).
[4] G. L. Cramp, A. M. Docking, S. Ghosh, and J. N. Coupland, Food Hydrocolloids **18**, 899 (2004).
[5] R. Montenegro, M. Antonietti, Y. Mastai, and K. Landfester, J. Phys. Chem. B **107**, 5088 (2003).
[6] R. Montenegro and K. Landfester, Langmuir **19**, 5996 (2003).
[7] I. Gülseren and J. Coupland, *Journal of the American Oil Chemists' Society*, J. Am. Oil Chem. Soc. **84**, 621 (2007).
[8] I. Gülseren and J. N. Coupland, J. Am. Oil Chem. Soc. **85**, 413 (2008).
[9] C. Lin, G. He, C. Dong, H. Liu, G. Xiao, and Y. Liu, Langmuir **24**, 5291 (2008).
[10] E. Dickinson, D. J. McClements, and M. J. W. Povey, J. Colloid Interface Sci. **142**, 103 (1991).
[11] D. J. McClements, E. Dickinson, S. R. Dungan, J. E. Kinsella, J. G. Ma, and M. J. W. Povey, J. Colloid Interface Sci. **160**, 293 (1993).
[12] E. Dickinson, F. J. Kruizinga, M. J. W. Povey, and M. van der Molen, Colloids Surf., A **81**, 273 (1993).
[13] D. J. McClements, S. R. Dungan, J. B. German, C. Simoneau, and J. E. Kinsella, J. Food Sci. **58**, 1148 (1993).
[14] Y. Shinohara, N. Kawasaki, S. Ueno, I. Kobayashi, M. Nakajima, and Y. Amemiya, Phys. Rev. Lett. **94**, 097801 (2005).
[15] Y. Shinohara, T. Takamizawa, S. Ueno, K. Sato, I. Kobayashi, M. Nakajima, and Y. Amemiya, Cryst. Growth Des. **8**, 3123 (2008).
[16] M. L. Schlossman and A. M. Tikhonov, *Annual Review of Physical Chemistry*, Annu. Rev. Phys. Chem. **59**, 153 (2008).
[17] V. Klang, N. B. Matsko, C. Valenta, and F. Hofer, Micron **43**, 85 (2012).
[18] H. B. de Aguiar, M. L. Strader, A. G. F. de Beer, and S. Roke, J. Phys. Chem. B **115**, 2970 (2011).
[19] H. B. de Aguiar, J.-S. Samson, and S. Roke, Chem. Phys. Lett. **512**, 76 (2011).
[20] A. G. F. de Beer and S. Roke, J. Chem. Phys. **132**, 234702 (2010).
[21] S. Roke and G. Gonella, Annu. Rev. Phys. Chem. **63**, 353 (2012).
[22] Note, See Supplemental Material at [URL to be inserted] for details on the sum-frequency scattering technique and the fitting of the spectra.

[23] J. Wang, H. Dubost, A. Ghalgaoui, W. Zheng, S. Carrez, A. Ouvrard, and B. Bourguignon, Surf. Sci. **626**, 26 (2014).

[24] B. E. A. Saleh and M. C. Teich, *Fundamentals of photonics*, 2nd ed. (Wiley, 2007) p. 89.

[25] A. G. F. de Beer, S. Roke, and J. I. Dadap, J. Opt. Soc. Am. B **28**, 1374 (2011).

[26] D. K. Hore, M. Y. Hamamoto, and G. L. Richmond, J. Chem. Phys. **121**, 12589 (2004).

[27] T. Delmas, H. Piraux, A.-C. Couffin, I. Texier, F. Vinet, P. Poulin, M. E. Cates, and J. Bibette, *Langmuir*, Langmuir **27**, 1683 (2011).

[28] D. R. Lide, ed., *CRC Handbook of Chemistry and Physics*, 88th ed. (CRC Press, 2007).

[29] N. Michel, A.-S. Fabiano, A. Polidori, R. Jack, and B. Pucci, Chem. Phys. Lipids **139**, 11 (2006).

[30] Y. M. S. Micheletto, N. P. da Silveira, D. M. Barboza, M. C. dos Santos, V. R. de Lima, F. C. Giacomelli, J. C. V. Martinez, T. E. A. Frizon, and A. G. Dal Bó, Colloids Surf., A **467**, 166 (2015).

[31] R. P. Sear, J. Phys.: Condens. Matter **19**, 033101 (2007).

[32] D. J. McClements, E. Dickinson, and M. J. W. Povey, Chem. Phys. Lett. **172**, 449 (1990).

[33] H.-F. Wang, W. Gan, R. Lu, Y. Rao, and B.-H. Wu, Int. Rev. Phys. Chem. **24**, 191 (2005).

[34] Y. Chen, K. C. Jena, and S. Roke, J. Phys. Chem. C **119**, 17725 (2015).

[35] R. A. MacPhail, H. L. Strauss, R. G. Snyder, and C. A. Elliger, J. Phys. Chem. **88**, 334 (1984).

[36] G. Sefler, Q. Du, P. Miranda, and Y. Shen, Chem. Phys. Lett. **235**, 347 (1995).

[37] R. Lu, W. Gan, B.-h. Wu, H. Chen, and H.-f. Wang, *The Journal of Physical Chemistry B*, J. Phys. Chem. B **108**, 7297 (2004).

[38] E. Tyrode and J. Hedberg, J. Phys. Chem. C **116**, 1080 (2012).

[39] C. D. Bain, J. Chem. Soc., Faraday Trans. **91**, 1281 (1995).

[40] R. G. Snyder, H. L. Strauss, and C. A. Elliger, J. Phys. Chem. **86**, 5145 (1982).

[41] J. C. Conboy, M. C. Messmer, and G. L. Richmond, Langmuir **14**, 6722 (1998).

[42] K. M. Wilkinson, L. Qunfang, and C. D. Bain, Soft Matter **2**, 66 (2006).

[43] O. Esenturk and R. A. Walker, J. Chem. Phys. **125**, 174701 (2006).

[44] P. Espeau, L. Roblès, D. Mondieig, Y. Haget, M. A. Cuevas-Diarte, and H. A. J. Oonk, J. Chim. Phys. **93**, 1217 (1996).

[45] X.-Y. Liu and P. Bennema, J. Cryst. Growth **135**, 209 (1994).

[46] A. G. F. de Beer and S. Roke, Phys. Rev. B **79**, 155420 (2009).

[47] A. G. F. de Beer, H. B. de Aguiar, J. F. W. Nijsen, and S. Roke, Phys. Rev. Lett. **102**, 095502 (2009).

[48] K. Nanjundiah and A. Dhinojwala, Phys. Rev. Lett. **95**, 154301 (2005).

[49] H. Saito, A. Kawagishi, M. Tanaka, T. Tanimoto, S. Okada, H. Komatsu, and T. Handa, J. Colloid Interface Sci. **219**, 129 (1999).

[50] J. I. Dadap, H. B. de Aguiar, and S. Roke, J. Chem. Phys. **130**, 214710 (2009).

[51] A. Nesje and S. O. Dahl, *Glaciers and Environmental Change* (Edward Arnold, 2000) p. 50.

[52] A. A. Schaerer, C. J. Busso, A. E. Smith, and L. B. Skinner, *Journal of the American Chemical Society*, J. Am. Chem. Soc. **77**, 2017 (1955).

[53] D. M. Small, *The Physical Chemistry of Lipids: From Alkanes to Phospholipids. Handbook of Lipid Res. 4* (Plenum Press, 1986) p. 30.